Journal of the Association of Arab Universities for Basic and Applied Sciences (2013) **14**, 51–59

University of Bahrain
Journal of the Association of Arab Universities for Basic and Applied Sciences
www.elsevier.com/locate/jaaubas
www.sciencedirect.com

ORIGINAL ARTICLE

Removal of two textile dyes from aqueous solutions onto calcined bones

Mohammadine El Haddad [a,b,*], Rachid Slimani [b], Rachid Mamouni [c], Saïd ElAntri [b], Saïd Lazar [b]

[a] *Equipe de Chimie Analytique & Environnement, Faculté Poly-disciplinaire, Université Cadi Ayyad, BP 4162, 46000 Safi, Morocco*
[b] *Laboratoire de Biochimie, Environnement & Agroalimentaire, Faculté des Sciences & Techniques, Université Hassan II, BP 146, 20800 Mohammedia, Morocco*
[c] *Laboratoire de Chimie Organique, Equipe de Chimie Bio-Organique Appliquée, Faculté des Sciences, Université Ibn Zohr, BP 8061, 80000 Agadir, Morocco*

Received 1 August 2012; revised 21 December 2012; accepted 3 March 2013
Available online 31 March 2013

KEYWORDS
Calcined bones;
Textile dyes;
Adsorption;
Kinetics;
Thermodynamic studies

Abstract The adsorption of textile dyes such as Direct Red 75 and Direct Red 80 onto calcined bone was studied for their removal from aqueous solutions. The adsorption of Direct Red 75 and Direct Red 80 occurred by studying the effects of adsorbent amount, dye concentration, contact time, pH media and temperature. The adsorption rate data were analyzed using the intraparticle diffusion model, pseudo first order and the pseudo second order kinetic models to determine adsorption rate constants. The isotherms of adsorption data were analyzed by various adsorption isotherm models such as Langmuir, Freundlich and Tempkin. All results found concluded that calcined bone could be effectively employed as an effective new low cost adsorbent for the removal of textile dyes from aqueous solutions.

1. Introduction

Environmental compliance requirements have become increasingly difficult to attain in both wastewater discharge and chemical handling. Dyes are widely used in industries such as textiles, leather, paper, and plastics to color their final products. Wastewater containing even a small amount of dyes can severely affect the aquatic life due to the reduction of light penetration and their toxicity (Mamdouh and El-Geundi, 1991). Many dyes and color effluents are toxic and have carcinogenic and mutagenic effects that influence environment and also human. Dye removal from wastewater effluent is a major environmental problem because of the difficulty of treating

* Corresponding author at: Equipe de Chimie Analytique & Environnement, Faculté Poly-disciplinaire, Université Cadi Ayyad, BP 1462, 46000 Safi, Morocco. Tel.: +212 6 64 51 80 40; fax: +212 524 669 516.
E-mail address: elhaddad71@gmail.com (M. El Haddad).
Peer review under responsibility of University of Bahrain.

ELSEVIER Production and hosting by Elsevier

1815-3852 © 2013 University of Bahrain. Production and hosting by Elsevier B.V. All rights reserved.
http://dx.doi.org/10.1016/j.jaubas.2013.03.002

such streams by conventional physical, chemical, physico-chemical and biological treatment methods. Many physical and chemical treatment methods including adsorption, coagulation, precipitation, filtration, electrodialysis, membrane separation and oxidation have been used for the treatment of dye-containing effluents (Morais et al., 1999; Chiou and Li, 2002).

Color removal from effluents polluted with dyes of textile industries has been considered a challenge due to the difficulty of treating such wastewaters by conventional methods. The effluents of the manufacturing and textile industries are discarded into rivers and lakes, changing their biological life. Adsorption process is one of the most effective and economically feasible methods for the removal of dyes from aqueous solutions.

The high cost of activated carbon sometimes makes its use limited. So many researchers have tried to search for alternative materials, which are relatively inexpensive, and at the same time with reasonable adsorptive efficiency. The use of clean methods of low priced and biodegradable adsorbents could be a good tool to minimize the environmental impact caused by textile effluents. Currently, because of their low cost and easy access, adsorption processes have been studied. This is the favorable technique for treatments of textile effluents. Different methods using low cost adsorbents for dye removal have been developed successfully. Various techniques such as adsorption (Arami et al., 2005, 2006), nanophotocatalysis (Mahmoodi et al., 2005, 2006, 2007), electrochemical (Fernandes et al., 2004), membrane processes (Akbari et al., 2002) have been used for the removal of organics as well as inorganics from research of the recent years mainly focused on utilizing natural materials as alternatives to activated carbon. The non degradable nature of dyes and their stability toward light and oxidizing agents complicate the selection of a suitable method for their removal. In comparison to the removal methods of colors, it has been well established that adsorption is the most convenient and effective technique to remove color from wastewater (Ravikumar et al., 2007). Adsorption is considered to be relatively superior to other techniques because of its low cost, simplicity of design, high efficiency, availability and ability to separate wide range of chemical compounds (Kannan and Sundaram, Ho, 2001; Meshko et al., 2001). It is considered that one of the major challenges faced with adsorption by activated carbon is its cost effectiveness. So, the research of the recent years mainly focused on utilizing natural materials as alternatives to activated carbon (Annadurai et al., 2002; EL-Geundi, 1997; Mall et al., 2005). Several natural adsorbents such as peat (Ho and McKay, 1998), banana peel (Annadurai et al., 2002), orange peel (Sivaraj et al., 2001), eucalyptus bark (Morais et al., 1999), Citrus waste biomass (Asgher and Bhatti, 2012), rice husk (Safa and Bhatti, 2011), barley husk (Haq et al., 2011), Citrus sinensis bagasse (Bhatti et al., 2012) and gasse pith (Chen et al., 2001) are some of the waste materials which have been tried for this purpose. Recently, we have used the animal bone meal to remove Basic Red 12 from aqueous solutions (El Haddad et al., 2012).

The present study was intended to remove Direct Red 75 and Direct Red 80 dyes from aqueous solutions using naturally prepared calcined bones as a new low cost adsorbent. The effect of various parameters like, adsorbent amount, dye concentration, contact time, pH, temperature, kinetics, equilibrium and thermodynamic studies was investigated.

2. Materials and methods

Animal Bones were collected from nearby butcher shops. All of the attached meat and fat were removed and cleaned from the bones. The bones were then washed several times with tap water and left in open air for several days to get rid of odors. Later, they were transferred to oven at 80 °C for drying. The dried bones were crushed and milled into different particle sizes in the range of 45–200 μm then calcined for 2 h at 800 °C. The residue was washed with water and was used after drying for 24 h at 80 °C. The residue was washed with water and was dried overnight at 100 °C in a conventional drying oven, and then calcined at a heating rate of 2 °C/min to 400 °C and kept at this temperature for 4 h until obtention of constant weight. The resulting material was denominated as calcined bones (CB).

Direct Red 75 (DR_{75}) and Direct Red 80 (DR_{80}) were chosen as organic anionic dyes in this study. The chemical structure of dyes DR_{75} and DR_{80} is shown in Fig. 1. Colored solutions were prepared by dissolving requisite quantity of each dye in distilled water. The final volume prepared was 500 mL. Adsorption studies for the evaluation of CB adsorbent for the removal of DR_{75} and DR_{80} dyes from aqueous solutions were carried out in triplicate using a batch contact adsorption method. Adsorption experiments were carried out with an initial concentration of 100 mg/L, amount of CB 1.2 g/L, pH from 2 to 12 and temperature from 25 °C to 70 °C. The pH was adjusted to a given value by the addition of 1 mol/L of HCl or NaOH and was measured using a Basic 20+ model pH-meter. All dye solutions prepared were filtered by Millipore membrane type 0.45 μm HA, and the concentrations of dyes were determined from its UV–Vis absorbance characteristic with the calibration method. A BioMate 6, UV/Visible spectrophotometer was used. Identification of CB was carried out by X-ray diffraction (Philips X'Pert PRO) and IR spectroscopy (spectrometer Bruker-Tensor 27).

The point of zero charge (pH_{pzc}) of the adsorbent was determined by adding 20 mL of 5.10^{-2} mol/L NaCl to several 50 mL cylindrical high-density polystyrene flasks (height 117 mm and diameter 30 mm). A range of initial pH (pH_i)

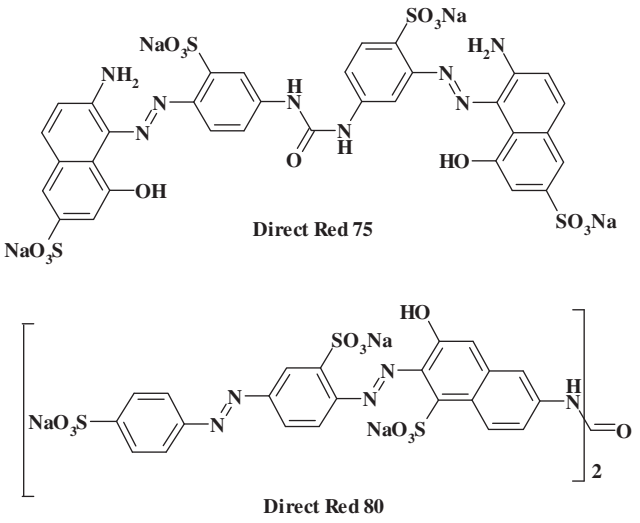

Figure 1 Chemical structure of textile dyes.

values of the NaCl solutions were adjusted from 2 to 10 by adding 10^{-1} mol/L of HCl and NaOH. The total volume of the solution in each flask was brought to exactly 30 mL by further addition of 5.10^{-2} mol/L NaCL solution. The pH_i values of the solutions were then accurately noted and 50 mg of each adsorbent was added to each flask, which was securely capped immediately. The suspensions were shaken in a shaker at 298 K and allowed to equilibrate for 48 h. The suspensions were then centrifuged at 3600 rpm for 10 min and the final pH (pH_f) values of the supernatant liquid were recorded. The value of pH_{pzc} is the point where the curve of ΔpH (pH_f–pH_i) versus pH_i crosses the line equal to zero (Calvete et al., 2009). The surface analysis was carried out with a volumetric adsorption analyzer, ASAP 2020, from Micromeritrics, at 77 K (boiling point of nitrogen). The samples were pretreated at 473 K for 24 h under a nitrogen atmosphere in order to eliminate the moisture adsorbed on the solid sample surface and obtaining a constant weight. After, the samples were submitted to 298 K in vacuum, reaching the residual pressure of 10^{-4} Pa (Calvete et al., 2010).

3. Results and discussion

3.1. Characterization of CB adsorbent

Elemental analysis of ABM shows a high yield of Ca (49.62%) and P (42.36%) with a (Ca/P) ratio equal to 1.17. Small amounts of Si (3.88%), Mg (1.32%), Na (0.77%), Al (0.35%), Fe (0.24%), Cl (0.24%), S (0.11%), K (0.07%), Sr (0.03%), Cu (0,03%) and Zn (0.02%) are found. An FTIR spectrum was carried out by encapsulation 0.5 mg of finely powder with 400 mg of KBr to get translucent disk. Carbonate is the most abundant substitution in bone mineral and according to its crystal position, carbonate apatite is designated as type A (OH^-) or type B (PO_4^{3-}), the latter being the most frequent bone (Best et al., 2008 and Landi et al., 2003). It is recognized that hydroxyapatite is derived from natural bone (Tadic and Epple, 2004; Figueiredo et al., 2009). FTIR spectrum of CB shows the characteristic bands of hydroxyapatite (571, 603, 962 (shoulder), 1047, and 1091 (shoulder) cm^{-1} due to phosphate vibrations and collagen (C=O stretching vibration at 1635 cm^{-1}, N–H in plane bending at 1458 cm^{-1}, C–H and N–H stretching modes in 3000–3571 cm^{-1} region) (Mkukuma et al., 2004; Paschalis et al., 1997; Rehman and Bonfield, 1997). Additionally, the typical bands of carbonate substituting for phosphate site (type B) in the apatite lattice are also observed: band at 874 cm^{-1} and double bands at 1385/1445 cm^{-1} (Murugan et al., 2006; Haberko et al., 2006). The diffractogram of CB shows only the characteristic pattern of hydroxyapatite. These results confirm that the amorphous organic component was removed after calcinations as found in the literature (Figueiredo et al., 2010). For 2θ between 25° and 45°, the main lattice reflections originate peaks at 25°, 28.1°, 32.8°, 33.7°, 34.5°, and 39.7° being respectively assigned to the (002), (102), (210), (211), (112), and (300) Miller plans of hydroxyapatite (Figueiredo et al., 2010). The specific surface area of CB was determined by BET method from adsorption–desorption isotherm of nitrogen at its liquid temperature 77 K and was found to be S_p = 85 m^2/g. We have already used this support as catalyst for the organic compound synthesis (Riadi et al., 2010, 2011; Mamouni et al., 2010).

3.2. Effect of CB adsorbent weight on dye removal

The study of CB adsorbent mass for the removal of DR_{75} and DR_{80} dyes from aqueous solutions was carried out using CB adsorbent mass ranging from 0.6 g to 1.6 g. The effect of CB mass on adsorbed amount of each adsorbed was investigated by contacting 200 mL of dye solution with an initial concentration of 50 mg/L using jar test at room temperature 25 °C at initial pH solutions for 60 min. Different amounts of CB (0.6, 0.8, 1, 1.2, and 1.6 g) in 200 mL for both solution dyes DR_{75} and DR_{80} were applied. After equilibrium, the samples were centrifuged and the concentration in the supernatant dye solution was analyzed. The plots of dye removal percentage versus time at different adsorbent amounts are shown in Fig. 2. Increases in the percentage of the dye removal versus the increasing time and adsorbent amounts could be attributed to increases in the adsorbent surface areas, increasing the number of adsorption sites available for adsorption, as already reported in several papers (Cardoso et al., 2011; Deniz and Karaman, 2011 and Safa and Bhatti, 2011). Adsorption increases from 61% to 89% through 5 min to 60 min for DR_{75} and from 56% to 84% through 5 min to 60 min for DR_{80}. We note that DR_{75} and DR_{80} have the same behavior versus CB.

3.3. Effect of dye concentration on dye removal by CB

A specific weight of CB adsorbent (1 g) with 50 mL of DR_{75} and DR_{80} dyes solutions was kept constant for the batch experiments. Initial DR_{75} and DR_{80} solutions of 25, 50, 75, and 100 mg/L were performed at 25 °C on a magnetic stirrer

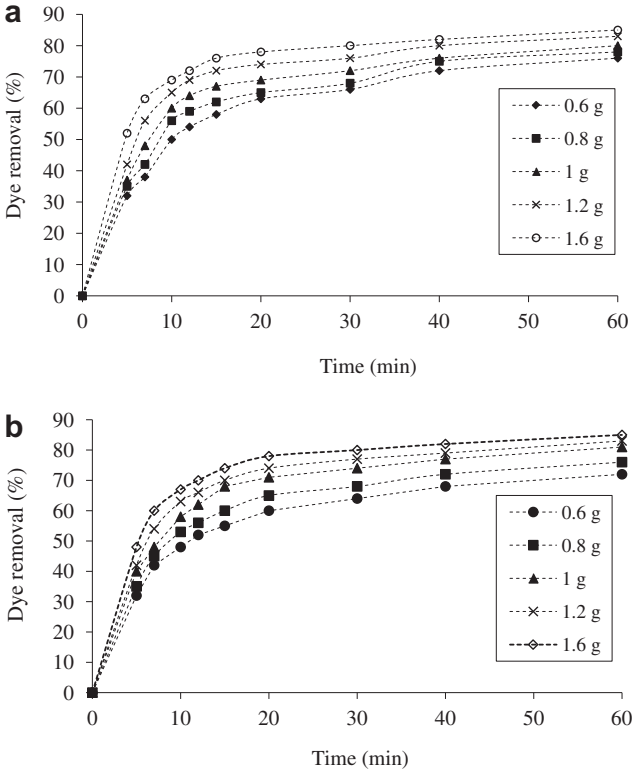

Figure 2 Effect of adsorbent amounts on dye removal by CB (a) DR_{75} (b) DR_{80}.

operated at 250 rpm for 1 h. Results of this study are shown in Fig. 3. It can be seen that the removal of dye initially increases with the increase of the concentration achieving the maximum removal of 50% at 25 mg/L and of 80% for 100 mg/L for DR_{80} and about 45% of removal dye at 25 mg/L and of 80% for 100 mg/L for DR_{75}. This greater initial adsorption with higher initial dye concentrations might be explained by the active site availability of the adsorbent. Opposite results are shown using removal dye on another adsorbent (Mahmoodi et al., 2011).

3.4. Effect of pH

One of the main variables affecting the adsorption process is pH, influencing not only the surface charge of adsorbent, the degree of ionization of the material present in the solution and the dissociation of functional groups on the active sites of the adsorbent, but also the solution dye chemistry. In this fact, pH must control the adsorption of dyes onto suspended particles, because both adsorbed molecules and adsorbent particles may have functional groups which are affected by the concentration of H^+ ions in the solution and which are involved in the molecular adsorption process at the active sites of adsorbent. Firstly, the results of blank dye solution studies indicate that the change of the initial pH 2–12 of dye solution has a negligible effect on the λ_{max} of DR_{75} and DR_{80} dyes. This observation proves that any chemical structural change of dye molecules is not occurred at pH 2–12. The maximum absorbance wavelength λ_{max} (nm) of DR_{75} and DR_{80} at different pH values is shown in Table 1. The pH of the zero charge of the CB is determined to be 8.4, for pH values higher than 8.4, the surface of the CB becomes negatively charged and this is opposite for pH < 8.4.

From Fig. 4, it can be seen that the amount of dye adsorbed on the CB is high for pH between 3 and 8.4, which indicates that the positive form of CB is responsible for adsorption in this range. For basic pH, the decrease of the amount of adsorbed dye molecules is prevented by the repulsive electrostatic forces existing between the negative charged surface of CB and $Ph\text{-}SO_3^-$ groups of the dye predominant in this range of pH. The removal dye % uptake decreased from 87% at pH 2% to 29% at pH 12 for DR_{75} and from 84% at pH 2% to 24% at pH 12 for DR_{80}. The decrease of the amount of adsorption below pH 3 can be due to the ionization of the amine and amide groups of the dye with H^+, which leads the molecules of the dye to be positively charged. The repulsive electrostatic forces of dye molecules positively charged with the positively charged surface of the adsorbent increase. Consequently, adsorption decreases.

3.5. Effect of temperature

The temperature has two major effects on the adsorption process. Increasing the temperature is known to increase the rate of diffusion of the adsorbed molecules across the external boundary layer and the internal pores of the adsorbent particles, owing to the decrease in the viscosity of the solution. In addition, changing temperature will change the equilibrium

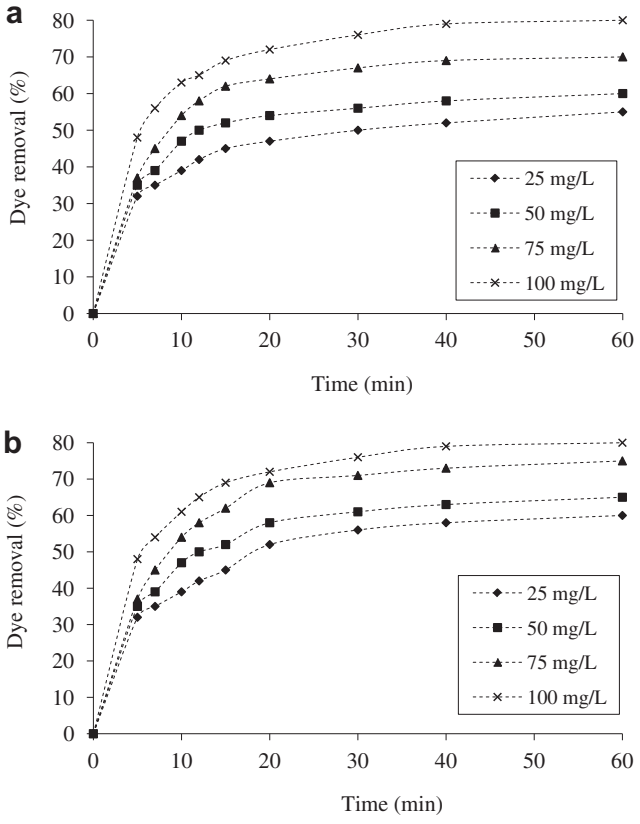

Figure 3 Effect of dye concentration on dye removal by CB (a) DR_{75} (b) DR_{80}.

Table 1 Effect of pH on the maximum absorbance wavelength λ_{max} (nm) of DR_{75} and DR_{80}.

pH	λ_{max} (nm)	
	DR_{75}	DR_{80}
2	521	541
4	521	531
6	522	528
8	522	532
10	521	532
12	521	537

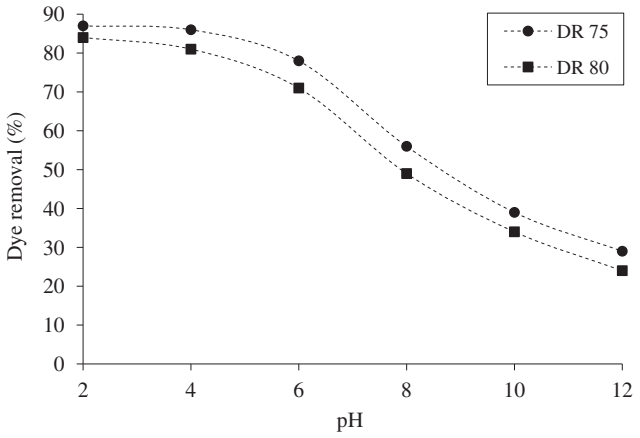

Figure 4 Effect of pH on dye removal by CB.

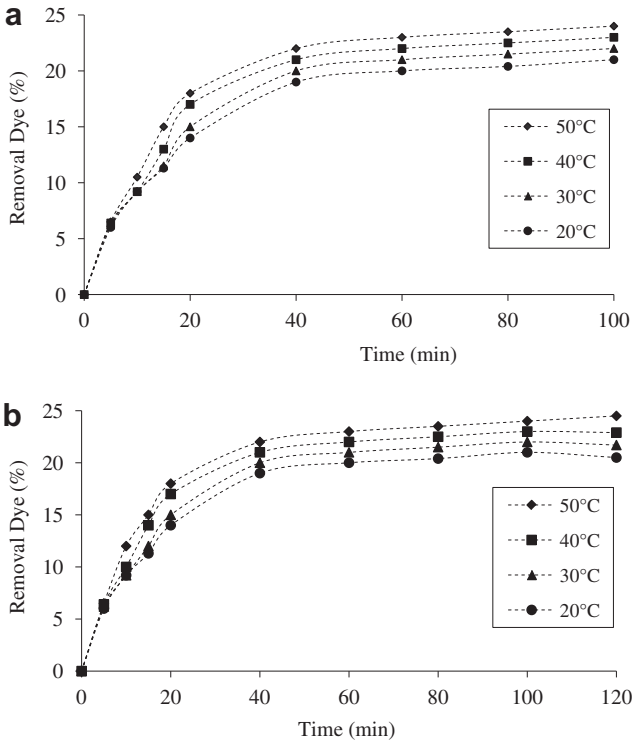

Figure 5 Effect of temperature on the kinetics of adsorption of DR_{75} and DR_{80} onto CB.

capacity of the adsorbent for a particular adsorbate. Fig. 5 shows the results of experiments carried out at different solution temperatures. The removal of DR_{75} increases from 22.31 mg/g to 24.23 mg/g and for DR_{80} from 20.95 mg/g to 23.89 mg/g by increasing the temperature of the solution from 20 °C to 50 °C, indicating that the process to be endothermic. This kind of temperature dependence of the amount of the dye adsorbed may be due to a possible mechanism of interaction between the sulfonyl groups of dyes and the cationic sites of CB where such a reaction could be favored at higher temperatures.

3.6. Adsorption kinetics

Several models can be used to express the mechanism of analyte adsorption onto adsorbent. In order to describe a fat and effective model, investigations were made on adsorption rate. For the examination of the controlling mechanisms of adsorption process, such as chemical reaction, diffusion model control and mass transfer, several kinetic models are used to test the experimental data (Weber and Morris, 1963; Lagergren, 1898; Ho, 2001).

To explore the possibility of intraparticle diffusion resistance affecting adsorption, it was necessary to use intraparticle diffusion model as (Weber and Morris, 1963):

$$q_t = k_p t^{\frac{1}{2}} + I \tag{1}$$

where q_t, k_p and I are amount of dye adsorbent (mg/g) at time t (mn), the intraparticle diffusion model rate constant (mg/g $mn^{1/2}$) and the intercept, respectively. Values of I give an idea about the thickness of the boundary layer. According to this model, the plot of uptake should be linear if intraparticle diffusion is involved in the adsorption process and if these lines pass through the origin then intraparticle diffusion is the rate controlling step (Weber and Morris, 1963). When the plots do not pass through the origin, this is indicative of some degree of boundary layer control. This further shows that the intraparticle diffusion is not the only rate limiting step, but also other kinetic models may control the rate of adsorption.

Pseudo-first order equation is generally represented as follows (Lagergren, 1898):

$$\frac{dq_t}{dt} = k_1(q_e - q_t) \tag{2}$$

where q_e and k_1 are the amount of dye adsorbed at equilibrium (mg/g) and the equilibrium rate constant of pseudo-first order kinetics (mn^{-1}), respectively. After integration by applying conditions, $q_t = 0$ at $t = 0$ and $q_t = q_t$ at $t = t$, then Eq. (2) becomes:

$$\log(q_e - q_t) = \log q_e - \frac{k_1}{2.303} t \tag{3}$$

Data were applied to be the pseudo-second order kinetic which is expressed as:

$$\frac{dq_t}{dt} = k_2(q_e - q_t)^2 \tag{4}$$

where k_2 is the equilibrium rate constant of pseudo-second order (g/mg mn). On integrating the Eqs. (4) and (5) is obtained.

$$\frac{t}{q_t} = \frac{1}{k_2 q_e^2} + \frac{1}{q_e} t \tag{5}$$

To understand the applicability of the model linear plots of t/q_t versus t at different dye concentration values (25, 50, 75, and 100 mg/L) for the adsorption of dyes onto CB, we have plotted the graph of t/Qt versus t at differents concentrations and the results are shown in Fig. 6. The values of k_p, I, R_I^2 (correlation coefficient for intraparticle diffusion model), k_1, k_2, R_F^2 (correlation coefficient for pseudo-first order adsorption kinetics) and R_S^2 (correlation coefficient for pseudo-second order adsorption kinetics) were calculated and shown in Table 2. Adsorption kinetic data of dyes showed that the rates of adsorption followed pseudo-second order kinetics.

3.7. Adsorption isotherms

Equilibrium adsorption isotherm data were analyzed according to the Langmuir, Freundlich, and Tempkin models. The Langmuir equation is suitable to describe the adsorptive behavior of homogeneous surfaces. The Langmuir adsorption model is established on the following hypotheses: uniformly energetic adsorption sites, monolayer coverage, and no lateral interaction between adsorbed molecules. A mathematical expression of Langmuir can be written as (Langmuir, 1918):

$$q_e = \frac{Q_0 K_L C_e}{1 + K_L C_e} \tag{6}$$

where q_e (mg/g) is the adsorbed amount at equilibrium, C_e is the equilibrium concentration of the adsorbate (mg/L), K_L is Langmuir equilibrium constant (L/mg) and Q_0 the maximum adsorption capacity (mg/g). The linear form of Langmuir equation is:

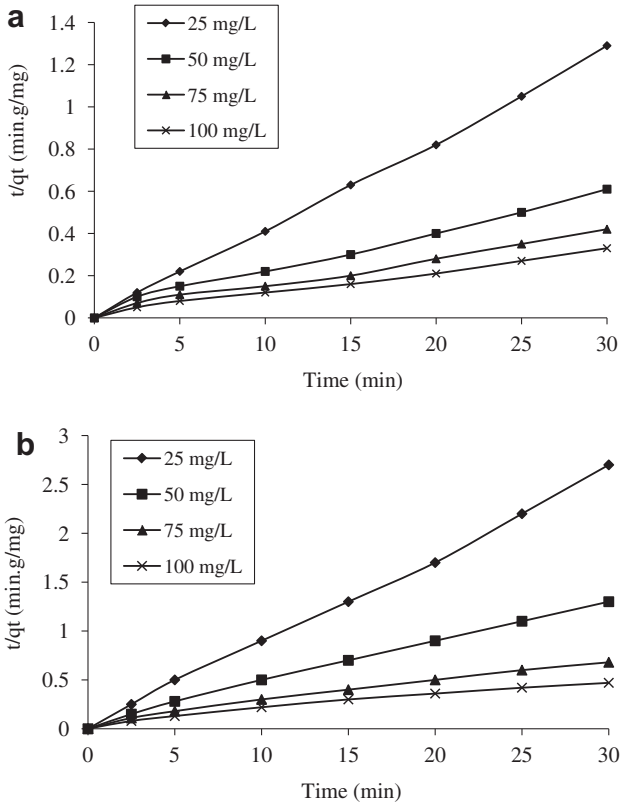

Figure 6 Pseudo-second order adsorption kinetics of dyes on CB (a) DR_{75}, (b) DR_{80}.

$$\frac{C_e}{q_e} = \frac{1}{K_L Q_0} + \frac{C_e}{Q_0} \tag{7}$$

The essential characteristic of Langmuir isotherm can be expressed by the dimensionless constant called equilibrium parameter, R_L, defined by:

$$R_L = \frac{1}{1 + K_L C_0} \tag{8}$$

where C_0 is the initial dye concentration (mg/L). R_L values indicate the type of isotherm to be irreversible ($R_L = 0$), favorable ($0 < R_L < 1$), and unfavorable ($R_L > 1$) (Mahmoodi and Arami, 2008).

The Freundlich isotherm endorses the heterogeneity of the surface and assumes that the adsorption occurs at sites with different energies of adsorption. The energy of adsorption varies as a function of the surface coverage (Freundlich, 1906). A mathematical expression of Freundlich isotherm was as follows:

$$q_e = K_F C_e^{1/n} \tag{9}$$

where K_F (L/mg) is Freundlich constant and n is the heterogeneity factor. The K_F value is related to the adsorption capacity; while the $1/n$ value is related to the adsorption intensity. $1/n$ values indicate the type of isotherm to be irreversible ($1/n = 0$), favorable ($0 < 1/n < 1$), unfavorable ($1/n > 1$) (Mahmoodi and Arami, 2008). Eq. (9) can be rearranged to linear form:

$$\log q_e = \log K_F + \frac{1}{n} \log C_e \tag{10}$$

Tempkin isotherm contains a factor that explicitly takes into account the adsorbing species adsorbent interactions. The Tempkin equation is given as (Tempkin and Pyzhev, 1940; Kim et al. 2004):

$$q_e = \frac{RT}{bLn(K_T C_e)} \tag{11}$$

This can be linearized as:

$$q_e = B_1 Ln K_T + B_1 Ln C_e \tag{12}$$

where:

$$B_1 = \frac{RT}{b} \tag{13}$$

Tempkin equation assumes that the heat of adsorption of all the molecules in the layer decreases linearly with coverage due to adsorbent–adsorbate interactions and the adsorption is characteristic by a uniform distribution of binding energies, up to some maximum energy (Tempkin and Pyzhev, 1940; Kim et al. 2004). A plot of q_e versus ln C_e enables the determination of the isotherm constants B_1 and K_T from the slope and the intercept, respectively. K_T is the equilibrium binding constant (L/mol) corresponding to the maximum binding energy and constant B_1 is related to the heat of adsorption. The Q_0, K_L, R_L, R_L^2 (correlation coefficient for Langmuir isotherm), K_F, n, R_F^2 (correlation coefficient for Freundlich isotherm), K_T, B_1, and R_T^2 (correlation coefficient for Tempkin isotherm) are given in Table 3. The results indicated that isotherm data of DR_{75} followed Langmuir isotherm and isotherm data of DR_{80} followed Freundlich isotherm models.

Table 2 Adsorption isotherm constants of DR_{75} and DR_{80} dyes onto CB.

Dye Concentration (mg/L)	$(q_e)_{exp}$	Intraparticle diffusion model	Pseudo-first order					Pseudo-second order		
		k_p	I	R_I^2	$(q_e)_{cal.}$	k_1	R_F^2	$(q_e)_{cal.}$	k_2	R_S^2
DR_{75}										
25	23.07	4.53	6.67	0.67	09.12	0.25	0.49	24.07	0.04	0.99
50	42.45	7.07	13.23	0.74	22.56	0.31	0.65	45.76	0.02	0.98
75	54.47	8.82	13.34	0.81	39.54	0.34	0.89	61.56	0.01	0.99
100	65.78	9.93	13.45	0.87	45.76	0.35	0.92	86.78	0.01	0.99
DR_{80}										
25	21.56	2.74	6.06	0.64	12.54	0.95	0.94	19.67	0.05	0.99
50	40.32	6.65	12.95	0.69	18.79	0.64	0.95	37.45	0.03	0.99
75	49.83	7.78	13.04	0.73	22.78	0.62	0.95	42.78	0.02	0.99
100	63.78	8.86	13.17	0.76	36.76	0.56	0.93	58.65	0.02	0.99

Table 3 Isotherm constants for dye adsorption at different temperatures onto CB.

Temperature (°C)	Langmuir isotherm model				Freundlich isotherm model			Tempkin isotherm model		
	Q_0	K_L	R_L	R_L^2	K_F	n	R_F^2	K_T	B_1	R_T^2
DR_{75}										
20	24.56	0.23	0.07	0.999	19.56	3.56	0.996	3.67	12.05	0.945
30	24.31	0.27	0.06	0.999	20.47	3.78	0.992	4.63	12.38	0.976
40	23.78	0.25	0.06	0.999	22.78	3.90	0.993	7.78	11.12	0.976
50	21.54	0.26	0.05	0.999	25.76	4.12	0.884	10.96	10.98	0.980
DR_{80}										
20	22.54	0.13	0.13	0.992	7.93	2.45	0.999	1.65	7.67	0.943
30	21.89	0.15	0.11	0.994	8.74	2.67	0.999	1.97	7.48	0.956
40	21.65	0.17	0.10	0.995	9.67	2.87	0.999	2.65	7.23	0.945
50	20.32	0.19	0.08	0.992	10.67	2.91	0.999	3.17	7.09	0.934

3.8. Thermodynamics studies

The thermodynamic data reflects the feasibility and favorability of the adsorption. The parameters such as free energy change ΔG^0, enthalpy change ΔH^0 and entropy change ΔS^0 can be estimated by the change of equilibrium constants with temperature. The free energy change of the adsorption reaction is given by: $\Delta G^0 = -RTLnK_C$where ΔG^0 is the free energy change (kj/mol), R is the universal gas constant (8.314 J/mol K), T is the absolute temperature K and K_C states the equilibrium constant (q_e/C_e). The values of ΔH^0 and ΔS^0 can be calculated from the Van't Hoff equation (Ozcan et al., 2006):

$$LnK_C = -\frac{\Delta H^0}{RT} + \frac{\Delta S^0}{R} \tag{14}$$

When K_C is plotted against $1/T$, a straight line with slope $-\Delta H^0/R$ and intercept $\Delta S^0/R$ are found. The calculated thermodynamic parameters are depicted in Table 4. In this study, ΔG^0 values were determined as −3.58 and −6.41 kJ/mol at 30 °C for DR_{75} and DR_{80} respectively. The negative values of ΔG^0 suggest that the adsorption of DR_{75} and DR_{80} onto CB is a highly favorable process. ΔH^0 values were obtained as 12.35 and 6.45 kJ/mol for DR_{75} and DR_{80} respectively. ΔS^0 values were obtained as 52.56 and 42.45 J/mol K for DR_{75} and DR_{80} respectively. The positive values of ΔH^0 show that the adsorption is endothermic process while positive ΔS^0 values reflect the increasing randomness at the solid/solution interface during the adsorption. The change in free energy for physical and chemical reactions is between −20 and 0 kJ/mol and −80 and −400 kJ/mol respectively (Ozcan et al., 2006). The values of ΔG^0 in Table 4 are within −20 and 0 kJ/mol indicating that the physical reaction is the dominating mechanism.

Table 4 Thermodynamic parameters of dye adsorption onto CB.

Temperature (°C)	Thermodynamic parameters		
	ΔG^0 (kJ/mol)	ΔH^0 (kJ/mol)	ΔS^0 (J/mol K)
DR_{75}			
20	−3.31	12.35	52.56
30	−3.58		
40	−4.10		
50	−4.63		
DR_{80}			
20	−6.20		
30	−6.41	6.45	42.45
40	−6.83		
50	−7.26		

4. Conclusion

The results indicated that CB is a promising new low cost adsorbent for removal of direct dyes DR_{75} and DR_{80} from aqueous solutions. The kinetic studies of dyes on CB indicated that the adsorption kinetics of dyes on CB followed the pseudo-second order at different dye concentration values. The equilibrium data have been analyzed. The results showed that the DR_{75} followed Langmuir isotherm and DR_{80} followed Freundlich isotherm models. Thermodynamic studies indicated that the dye adsorption onto CB was a spontaneous, endothermic and physical reaction.

References

Arami, M., Limaee, N.Y., Mahmoodi, N.M., Tabrizi, N.S., 2005. Removal of dyes from colored textile wastewater by orange peel adsorbent: equilibrium and kinetics studies. Journal of Colloid and Interface Science 288, 371–376.

Arami, M., Limaee, N.Y., Mahmoodi, N.M., Tabrizi, N.S., 2006. Equilibrium and kinetics studies for the adsorption of direct and acid dyes from aqueous solution by soy meal hull. Journal of Hazardous Materials 135, 171–179.

Akbari, A., Remigy, J.C., Aptel, P., 2002. Treatment of textile dye effluents using a polyamide-based nanofiltration membrane. Chemistry Engineering and Processing 41, 601–609.

Annadurai, G., Juang, R.S., Lee, D.J., 2002a. Use of cellulose-based wastes for adsorption of dyes from aqueous solutions. Journal of Hazardous Materials 92, 263–274.

Annadurai, G., Juang, R.S., Lee, D.J., 2002b. Factorial design analysis for adsorption of dye on activated carbon beads incorporated with calcium alginate. Advances in Environmental Research 6, 191–198.

Asgher, M., Bhatti, H.N., 2012. Evaluation of thermodynamics and effect of chemical treatments on sorption potential of citrus waste biomass for removal of anionic dyes from aqueous solutions. Ecological Engineering 38, 79–85.

Best, S.M., Porter, A.E., Thian, E.S., Huang, J., 2008. Bioceramics: Past, present and for the future. Journal of European Ceramic Society 28, 1319–1327.

Bhatti, H.N., Akhtar, N., Saleem, N., 2012. Adsorptive removal of methylene blue by low cost Citrus sinensis bagasse: equilibrium, kinetic and thermodynamic characterization. Arabian Journal of Science and Engineering 37, 9–18.

Calvete, T., Lima, E.C., Cardoso, N.F., Dias, S.L.P., Pavan, F.A., 2009. Applications of carbon adsorbents prepared from the Brazilian-pine fruit shell for removal of Procion Red MX 3B from aqueous solution – kinetic, equilibrium and thermodynamic studies. Chemical Engineering Journal 155, 627–636.

Calvete, T., Lima, E.C., Cardoso, N.F., Vaghetti, J.C.P., Dias, S.L.P., Pavan, F.A., 2010. Applications of carbon adsorbents prepared from the Brazilian-pine fruit shell for removal of reactive orange 16 from aqueous solution – kinetic, equilibrium and thermodynamic studies. Journal of Environmental Management 91, 1695–1706.

Cardoso, N.F., Pinto, R.B., Lima, E.C., Calvete, T., Amavisca, C.M., Royer, B., Cunha, M.L., Fernandes, T.H.M., Pinto, I.S., 2011. Removal of remazol black B textile dye from aqueous solution by adsorption. Desalination 269, 92–103.

Chen, B., Hui, C.W., McKay, G., 2001. Film-pore diffusion modelling and contact time optimization for the adsorption of dyestuffs on pith. Chemical Engineering Journal 84, 77–94.

Chiou, M.S., Li, H.Y., 2002. Equilibrium and kinetic modeling of adsorption of reactive dye on cross-linked chitosan beads. Journal of Hazardous Materials 93, 233–248.

Deniz, F., Karaman, S., 2011. Removal of Basic Red 46 dye from aqueous solution by pine tree leaves. Chemical Engineering Journal 170, 67–74.

El Haddad, M., Mamouni, R., Saffaj, N., Lazar, S., 2012. Removal of a cationic dye –Basic Red 12– from aqueous solutions by adsorption onto animal bone meal. Journal of the Association of Arab Universities for Basic and Applied Sciences 12, 48–54.

EL-Geundi, M.S., 1997. Adsorbents for industrial pollution control. Adsorption Science and Technology 15, 777–787.

Fernandes, A., Morao, A., Magrinho, M., Lopes, A., Goncalves, I., 2004. Electrochemical degradation of C. I. Acid Orange 7. Dyes and Pigments 61, 287–296.

Figueiredo, M., Henriques, J., Martins, G., Guerra, F., Judas, F., Figueiredo, H., 2009. Physicochemical characterization of biomaterials commonly used in dentistry as bone substitutes-comparison with human bone. Journal of Biomaterials Materials Research 92B, 409–419.

Figueiredo, M., Fernando, A., Martins, G., Freitas, J., Judas, F., Figueiredo, H., 2010. Effect of the calcination temperature on the composition and microstructure of hydroxyapatite derived from human and animal bone. Ceramic International 36, 2383–2393.

Freundlich, H.M.F., 1906. Uber die adsorption in lasugen. Zeitschrift fur Physikalische Chemie (Leipzig) 57A, 385–470.

Haberko, K., Bucko, M.M., Brzezin´ska-Miecznik, J., Haberko, M., Mozgawa, W., Panz, T., Pyda, A., Zarebski, J., 2006. Natural hydroxyapatite-its behaviour during heat treatment. Journal of European Ceramic Society 26, 537–542.

Haq, I., Bhatti, H.N., Asgher, M., 2011. Removal of solar red BA textile dye from aqueous solution by low cost barley husk: equilibrium, kinetic and thermodynamic study. Canadian Journal of Chemical Engineering 89, 593–600.

Ho, Y.S., 2001. Sorption studies of acid dye by mixed sorbents. Adsorption 7, 139–147.

Ho, Y.S., McKay, G., 1998. Sorption of dye from aqueous solution by peat. Chemical Engineering Journal 70, 115–124.

Kim, Y., Kim, C., Choi, I., Rengaraj, S., Yi, J., 2004. Arsenic removal using mesoporous alumina prepared via a templating method. Environmental Science and Technology 38, 924–931.

Kannan, N., Sundaram, M.M., 2001. Kinetics and mechanism of removal of methylene blue by adsorption on various carbons-a comparative study. Dyes and Pigments 51, 25–40.

Lagergren, S., 1898. About the theory of so-called adsorption of soluble substances. Kungliga Svenska Vetenskapsakademiens. Handlingar 24, 1–39.

Landi, E., Celotti, G., Logroscino, G., Tampieri, A., 2003. Carbonated hydroxyl-apatite as bone substitute. Journal of European Ceramic Society 23, 2931–2937.

Langmuir, I., 1918. The adsorption of gases on plane surfaces of glass, mica and platinum. Journal of American Chemical Society 40, 1361–1403.

Mahmoodi, N.M., Arami, M., Limaee, N.Y., Gharanjig, K., Ardejani, F.D., 2006. Decolorization and mineralization of textile dyes at solution bulk by heterogeneous nanophotocatalysis using immobilized nanoparticles of titanium dioxide. Colloids and Surfaces A: Physicochemical and Engineering Aspects 290, 125–131.

Mahmoodi, N.M., Arami, M., Limaee, N.Y., Tabrizi, N.S., 2005. Decolorization and aromatic ring degradation kinetics of Direct Red 80 by UV oxidation in the presence of hydrogen peroxide utilizing TiO_2 as a photocatalyst. Chemical Engineering Journal 112, 191–196.

Mahmoodi, N.M., Arami, M., Limaee, N.Y., 2006a. Photocatalytic degradation of triazinic ring-containing azo dye (Reactive Red 198) by using immobilized TiO_2 photoreactor: bench scale study. Journal of Hazardous Materials 133, 113–118.

Mahmoodi, N.M., Arami, M., Limaee, N.Y., Tabrizi, N.S., 2006b. Kinetics of heterogeneous photocatalytic degradation of reactive dyes in an immobilized TiO_2 photocatalytic reactor. Journal of Colloid and Interface Science 295, 159–164.

Mahmoodi, N.M., Arami, M., 2006. Bulk phase degradation of Acid Red 14 by nanophotocatalysis using immobilized titanium (IV) oxide nanoparticles. Journal of Photochemistry and Photobiology A: Chemistry 182, 60–66.

Mahmoodi, N.M., Arami, M., Limaee, N.Y., Gharanjig, K., Nourmohammadian, F., 2007a. Nanophotocatalysis using immobilized titanium dioxide nanoparticle. Degradation and mineralization of water containing organic pollutant: case study of Butachlor. Materials Research Bulletins 42, 797–806.

Mahmoodi, N.M., Limaee, N.Y., Arami, M., Borhany, S., Mohammad-Taheri, M., 2007b. Nanophotocatalysis using nanoparticles of Titania. Mineralization and finite element modelling of Solophenyl dye decolourization. Journal of Photochemistry and Photobiology A: Chemistry 189, 1–6.

Mahmoodi, N.M., Arami, M., Limaee, N.Y., Gharanjig, K., 2007c. Photocatalytic degradation of agricultural *N*-heterocyclic organic pollutants using immobilized nanoparticles of titania. Journal of Hazardous Materials 145, 65–71.

Mahmoodi, N.M., Hayati, B., Arami, M., Lan, C., 2011. Adsorption of textile dyes on pine cone from colored wastewater: kinetic, equilibrium and thermodynamic studies. Desalination 268, 117–125.

Mahmoodi, N.M., Arami, M., 2008. Modelling and sensitivity analysis of dyes adsorption onto natural adsorbent from colored textile wastewater. Journal of Applied Polymer Science 109, 4043–4048.

Mamdouh, N.M., El-Geundi, M.S., 1991. Comparative cost of color removal from textile effluents using natural adsorbents. Journal of Chemical Technology and Biotechnology 50, 257–264.

Mamouni, R., Riadi, Y., Abrouki, Y., El Haddad, M., Saffaj, N., El Antri, S., Routier, S., Guillaumet, G., Lazar, S., 2010. First animal bone meal (ABM) as a new catalyst in thia-Michael addition. Letters in Organic Chemistry 7 (3), 269–271.

Mall, I.D., Srivastava, V.C., Agarwal, N.K., Mishra, I.M., 2005. Removal of congo red from aqueous solution by bagasse fly ash and activated carbon: kinetic study and equilibrium isotherm analyses. Chemosphere 61, 492–501.

Meshko, V., Markovska, L., Mincheva, M., Rodrigues, A.E., 2001. Adsorption of basic dyes on granular activated carbon and natural zeolite. Water Research 35, 3357–3366.

Mkukuma, L.D., Skakle, J.M.S., Gibson, I.R., Imrie, C.T., Aspden, R.M., Hukins, D.W.L., 2004. Effect of the proportion of organic material in bone on thermal decomposition of bone mineral: an investigation of a variety of bones from different species using thermogravimetric analysis coupled to mass spectrometry, high-

temperature X-ray diffraction, and Fourier transform infrared spectroscopy. Calcified Tissue International 75, 321–328.

Morais, L.C., Freitas, O.M., Goncalves, E.P., Vasconcelos, L.T., Gonzaa Lez Bec, C.G, 1999. Reactive dyes removal from wastewaters by adsorption on eucalyptus bark: variables that define the process. Water Research 33, 979–988.

Murugan, R., Ramakrishna, S., Rao, K.P., 2006. Nanoporous hydroxy-carbonate apatite scaffold made of natural bone. Materials Letters 60, 2844–2847.

Ozcan, A., Oncu, E.M., Ozcan, A.S., 2006. Kinetics, isotherm and thermodynamic studies of adsorption of Acid Blue 193 from aqueous solutions onto natural sepiolite. Colloids and Surfaces A277, 90–97.

Paschalis, E.P., Betts, F., DiCarlo, E., Mendelsohn, R., Boskey, A.L., 1997. FTIR microspectroscopic analysis of normal human cortical and trabecular bone. Calcified Tissue International 61, 480–486.

Ravikumar, K., Krishnan, S., Ramalingam, S., Balu, K., 2007. Optimization of process variables by the application of response surface methodology for dye removal using a novel adsorbent. Dyes and Pigments 72, 66–74.

Rehman, I., Bonfield, W., 1997. Characterization of hydroxyapatite and carbonated apatite by photo acoustic FTIR spectroscopy. Journal of Materials Science: Materials in Medicine 8, 1–4.

Riadi, Y., Mamouni, R., Azzalou, R., El Haddad, M., Routier, S., Guillaumet, G., Lazar, S., 2011. An efficient and reusable heterogeneous catalyst animal bone meal for facile synthesis of benzimidazoles, benzoxazoles and benzothiazoles. Tetrahedron Letters 52, 3492–3495.

Riadi, Y., Mamouni, R., Boulahjar, R., El Haddad, M., Routier, S., Guillaumet, G., Lazar, S., 2010. Animal bone meal as an efficient catalyst for crossed-aldol condensation. Tetrahedron Letters 51, 6715–6717.

Safa, Y., Bhatti, H.N., 2011. Kinetic and thermodynamic modeling for the removal of Direct Red 31 and Direct Red 26 dyes from aquoeus solutions by rice husk. Desalination 273, 313–322.

Sivaraj, R., Namasivayam, C., Kadirvelu, K., 2001. Orange peel as an adsorbent in the removal of acid violet 17 (acid dye) from aqueous solutions. Waste Management 21, 105–110.

Tadic, D., Epple, M., 2004. A thorough physicochemical characterisation of 14 calcium phosphate-based bone substitution materials in comparison to natural bone. Biomaterials 25, 987–994.

Tempkin, M.J., Pyzhev, V., 1940. Recent modification to Langmuir isotherms. Acta Physicochim USSR 12, 217–222.

Weber, W.J., Morris, J.C., 1963. Kinetics of adsorption on carbon from solutions. Journal of the Sanitary Engineering Division ASCE (SA2) 89, 3–60.